THE ASTROPHYSICAL JOURNAL, 469:238–245, 1996 September 20

THE AQUILA SUPERSHELL: A REMNANT OF MULTIPLE SUPERNOVAE[1]

WITOLD MACIEJEWSKI,[2] EDWARD M. MURPHY,[3] FELIX J. LOCKMAN,[4] AND BLAIR D. SAVAGE[2]

Received 1995 November 27; accepted 1996 March 22

ABSTRACT

A large area surrounding the Aquila Supershell (GS 034−06+65) was mapped in the H I 21 cm emission line. The new data show that the structure consists of an irregular spherical shell about 5°.6 in diameter, which extends 9°.5 below the Galactic plane, and of a well-defined, massive cone at low latitudes, which connects to a molecular cloud in the Galactic plane through a narrow (20 pc wide) channel of reduced H I emission. The system probably lies at a distance of ∼3.3 kpc, which implies that the shell has a diameter of ∼320 pc and extends at least 550 pc into the Galactic halo.

We estimate that the swept-up mass in the shell is $6.0 \times 10^4\ M_\odot$ and the mass in the cone is $1.8 \times 10^5\ M_\odot$. The concentration of supernova remnants, star-forming regions, and H II regions in this direction implies that the Aquila Supershell is a remnant of multiple supernovae and that star formation activity persists in this region of the Galaxy. We estimate that the total energy of the events creating the remnant is $(1–5) \times 10^{52}$ ergs, which corresponds to 10–100 supernova explosions powering the system in 10^7 yr. It is possible that the W48 complex of H II regions has resulted from star formation induced by a shock wave related to the cone.

Subject headings: Galaxy: structure — ISM: bubbles — ISM: individual (Aquila Supershell) — radio lines: ISM — ISM: structure — ISM: supernova remnants

1. INTRODUCTION

Holes, shells, and arclike structures are common features of the H I distribution of our Galaxy (Heiles 1979, 1984). Their connection to the star formation processes plays an important role in the structure and evolution of the gaseous components of the Galactic disk and halo. Observations show that other spiral galaxies also have shells and holes in their H I disks. About 150 holes, with sizes ranging from 100 pc to 1 kpc, have been found in the nearby galaxies M31 and M33 (Brinks & Bajaja 1986; Deul & den Hartog 1990). There is a very large hole, 1.5 kpc in diameter, accompanied by an expanding shell in M101 (Kamphuis, Sancisi, & van der Hulst 1991).

While different theories have been developed to explain these phenomena, the most widely recognized theory ascribes them to the collective action of stellar winds and supernova (SN) explosions originating from OB associations (Tenorio-Tagle & Bodenheimer 1988). The activity in an OB association creates a bubble in the surrounding ISM that is filled with hot gas. The excess pressure inside the bubble provides kinetic energy to ambient gas collected in a shell around the bubble. After the remnant of SNs and stellar winds has expanded to a size comparable to the scale height of the Galactic disk, the upper part of the shell accelerates and becomes Rayleigh-Taylor unstable (McCray & Kafatos 1987; Mac Low & McCray 1988). A phenomenon called "blowout" can occur, resulting in an escape of the gas from the interior of the bubble into the halo. Much more energetic phenomena can result from collisions of high-velocity clouds with the Galactic disk (Tenorio-Tagle et al. 1987). All these concepts are closely related to the Galactic fountain theory (Shapiro & Field 1976), in which the gas is constantly being moved upward to the halo by energetic phenomena in the Galactic plane. In the halo, the gas cools and falls back onto the disk.

The vertical extent of remnants, the nature of their confinement to the Galactic disk, and the degree to which they are capable of "blowout" are of considerable importance in understanding the energetics of the ISM and the nature of the Galactic halo. Some years ago, Heiles (1979) and Koo, Heiles, & Reach (1992) observed "worms" of H I in heavily processed images of Galactic 21 cm surveys. These worms are ridges of enhanced H I emission that extend approximately perpendicular to the Galactic plane at low latitude. Heiles interpreted them as the walls of superbubbles, the top of which had been ejected or disrupted allowing hot gas from the bubble interior to flow directly into the Galactic halo. We decided to examine examples of these worms in detail by making new, more sensitive H I measurements of the well-defined shell candidate, GS 034−06+65 (Heiles 1979), which corresponds to the worm GW 35.8−2.2 (Koo et al. 1992). In this paper, we show that this worm is a part of an energetic supershell, probably originating from SN explosions that take place in the Sagittarius arm, 3.3 kpc from the Sun. We name the whole structure the Aquila Supershell and discuss its relationship to star formation activity at its base.

In § 2, we describe the observational techniques we used, and in § 3 we present the observed properties of the Aquila Supershell. In § 4, we derive mass, energy, and age of the remnant. In § 5, we present the objects related to the supershell and discuss the physical processes causing and accompanying the supershell formation. Our results and conclusions are summarized in § 6.

2. OBSERVATIONS

The observations were made with the 140 ft (43 m) telescope in Green Bank, WV, during 1990 August, 1991 August, and 1992 August, using a dual-polarization receiver

[1] Based on observations obtained at the National Radio Astronomy Observatory, which is a facility of the National Science Foundation, operated under cooperative agreement by Associated Universities, Inc.

[2] Department of Astronomy, University of Wisconsin, 475 North Charter Street, Madison, WI 53706-1582; witold@uwast.astro.wisc.edu, savage@madraf.astro.wisc.edu.

[3] National Radio Astronomy Observatory, 520 Edgemont Road, Charlottesville, VA 22903, and Department of Astronomy, University of Virginia; emurphy@saips.cv.nrao.edu.

[4] National Radio Astronomy Observatory, P.O. Box 2, Green Bank, WV 24944; jlockman@sadira.gb.nrao.edu.

that had a total system temperature of less than 20 K at the zenith. The telescope has an angular resolution of 21′ (FWHM) at 21 cm wavelength. Spectra cover the range −200 to 250 km s^{-1} with respect to the LSR at a velocity resolution of 1 km s^{-1}. Spectra from the two polarizations were scaled to the brightness temperature system of Williams (1973), they were combined, and a parabolic baseline was removed.

We measured the 21 cm line emission over Galactic longitudes $11° \leq l \leq 40°$ and Galactic latitudes $-15° \leq b \leq -0.°5$. We also mapped a smaller region at positive latitudes $1.°5 \leq b \leq 6.°7$ between longitudes 30° and 40°. Spectra were always taken every 10′ in latitude and, for most of the mapped region, every 10′ in Galactic longitude. Each position was observed for 20 s. The longitude spacing of the data for $11° < l < 22°$ varies with latitude about an average of 10.′3. These data were interpolated onto a 10′ grid using a model Gaussian beam, which accounts for the somewhat smoother look of that region.

In all, about 30,000 spectra were acquired. The result of the observations is a cube containing the values of brightness temperature as a function of Galactic longitude, Galactic latitude, and radial velocity. A plane of the cube at a constant velocity has 175 pixels in the longitude axis and 131 in latitude axis, with 10′ spacing between pixels in both coordinates. The spectra have been smoothed to 2 km s^{-1} using a Gaussian smoothing function. There are 201 planes in the cube along the velocity axis, each separated by 2 km s^{-1}, beginning at −200 km s^{-1}. Some areas of the cube are blanked because of incomplete coverage or bad data.

3. OBSERVED PROPERTIES OF THE AQUILA SUPERSHELL

Figure 1 (Plate 8) is a color image of the brightness temperature of H I emission in the 2 km s^{-1} wide velocity plane centered on 56 km s^{-1}. The entire observed region is displayed. To improve the contrast against the bright emission that peaks near the Galactic plane, the intensities were scaled by sin $|b|$ for this display. The most outstanding feature in Figure 1 is the Aquila Supershell, centered at $l = 35°$, $b = -6°$. The Aquila Supershell was detected in the Heiles (1979) survey, where it is named GS 034−06+65. However, note that with more precise values for the shell center and radial velocity, the designation should be GS 035−06+56. To avoid confusion, we will retain the designation of Heiles but will mostly refer to the structure as the Aquila Supershell. In all following descriptions, our usage of the words "above" and "below" refers to the absolute distance $|z|$ from the Galactic plane or, equivalently, to the direction in which gravity points (e.g., an object at $b = -5°$ is above the object at $b = -4°$).

Figure 2 (Plate 9) displays the H I column density data for 20 velocity planes, each 2 km s^{-1} wide, between 34 and 72 km s^{-1}. Each image is centered on the Aquila Supershell, and each image covers the region $30° < l < 40°$ and $-15° < b < -1°$. For display only, data are also multiplied by sin $|b|$. A distinct shell system of H I emission can be most clearly seen at velocities between 52 and 60 km s^{-1}. It appears to be composed of two parts: a cone with its apex in the Galactic plane and a spherical shell above the cone. The cone is centered at $l = 34.°9$, $b = -2.°5$, with its apex at $l = 34.°6$, $b = -1.°4$. The spherical shell above the cone is centered at $l = 34.°7$, $b = -6.°7$ and has a radius of approximately 2.°8. In order to visualize the structure of the cone/shell system, we refer the reader to Figure 3, where the supershell is displayed in a gray scale. The cone is a bright Λ shape in the upper part of the image, roughly at $33° < l < 37°$ and $-4° < b < -1°$. The shell is a gray ring in the lower part of the image.

Although best seen at velocities 52–60 km s^{-1}, the Aquila Supershell can be traced to a minimum velocity of 38 km s^{-1}. In this velocity plane on Figure 2, one can see a hole of minimum emissivity at $l = 34.°8$, $b = -6.°7$. The hole gets somewhat bigger as velocities increase. By 44 km s^{-1}, a shell can be distinguished surrounding the hole. The shell is roughly 2.°0 thick and has an outer radius of 2.°8. The shell becomes thinner and more distinct in the higher velocity images, but the outer radius does not increase. At 56 km s^{-1}, the shell extends to $b = -9.°5$. The "top" of the shell—i.e., its part most distant from the Galactic plane—is smooth and distinct at velocities 52–60 km s^{-1}, but at still higher velocities it gets fainter and appears to be broken into several clumps, suggesting that it has been disrupted. However, it is difficult to rule out confusion with unrelated H I as the cause of these irregularities. The most obvious irregularity of the shell is the gap at $l = 36.°2$, $b = -6.°3$, which appears on the 68 km s^{-1} image. At 72 km s^{-1}, the only feature in the general direction of the shell is a filament at $31° < l < 32°$, $-9° < b < -4°$. Its association with the supershell is uncertain. At still higher velocities, there is a small H I cloud, possibly connected to the shell, centered at $l = 35.°2$, $b = -6.°8$, from velocities 88 to 108 km s^{-1}, that is 1.°5 in diameter at 92 km s^{-1}. No H I emission is detected in the direction of the Aquila Supershell at velocities ≥110 km s^{-1}. There is no obvious rear wall of the shell.

We do not see any clear evidence for expansion of the shell. An expanding shell has a characteristic structure, with one wall at low velocity, a growing then waning ring, and the opposite wall at the highest velocity. We do not clearly detect the near or far walls of the shell. As the LSR velocity increases for images on Figure 2, the hole inside the shell gets bigger, the shell becomes more distinct, and then the emission from the shell fades irregularly. The outer radius of the shell remains almost unchanged throughout the entire velocity range over which the shell is visible. While confusion with unrelated gas could hide the two walls, it cannot explain the nearly invariant size of the outer radius with velocity. The visibility of the supershell over a wide range of velocities (38–72 km s^{-1}) is probably owing to a high turbulence of the emitting gas (∼15 km s^{-1} velocity dispersion). We also do not see any emission at velocities negative with respect to the LSR, which reconfirms the fact that the Aquila Supershell does not expand rapidly. If the shell was expanding, one should see a ring of H I emission on displays of velocity versus latitude at constant longitude. Such a ring seems to be present on the $l = 34°50'$ plane, but it does not persist at adjacent longitudes. Moreover, at other longitudes, the shell emission appears in a form of clumps elongated in the direction of velocity, which indicates turbulent motions. This leads us to assume, henceforth, that the Aquila Supershell does not expand parallel to the line of sight.

The part of the system that we call the "cone," which connects the shell and the lower latitude emission of the Galactic plane, is most clearly visible between 58 and 62 km s^{-1} in Figure 2. The right (lower longitude) lobe consists of two parts. The first one is visible in the planes 40–48 km s^{-1} and is centered at $l = 33.°7$, $b = -4.°7$. Its opening half angle is 14°. The second part is more distinct. It appears on

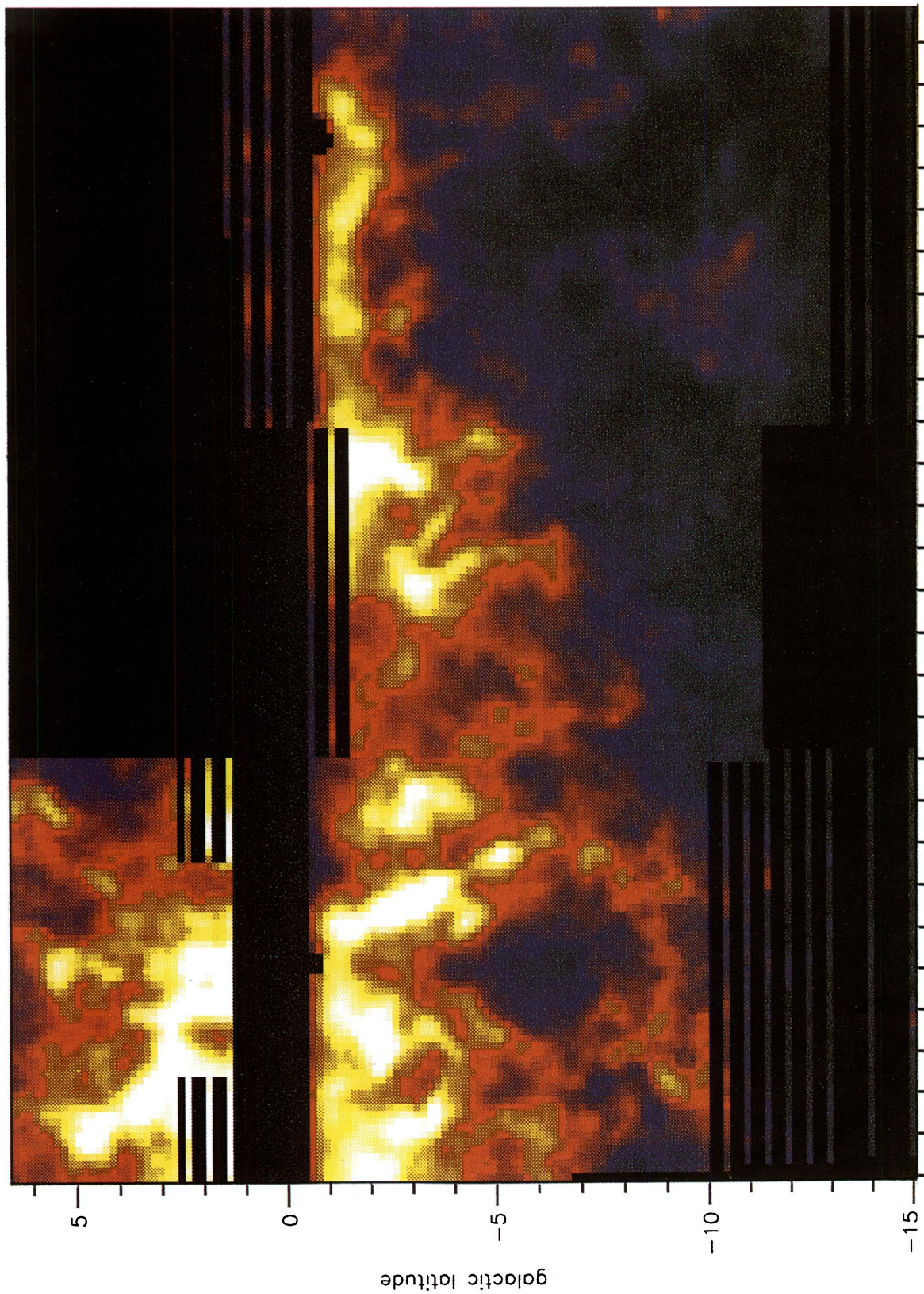

FIG. 1.—Color representation of H I brightness temperature of the entire observed region in a 2 km s^{-1} wide band at v_{LSR} = +56 km s^{-1}. Blank areas correspond to the lack of data. To increase the dynamic range of this figure, the H I intensities are multiplied by sin $|b|$.

MACIEJEWSKI et al. (see 469, 239)

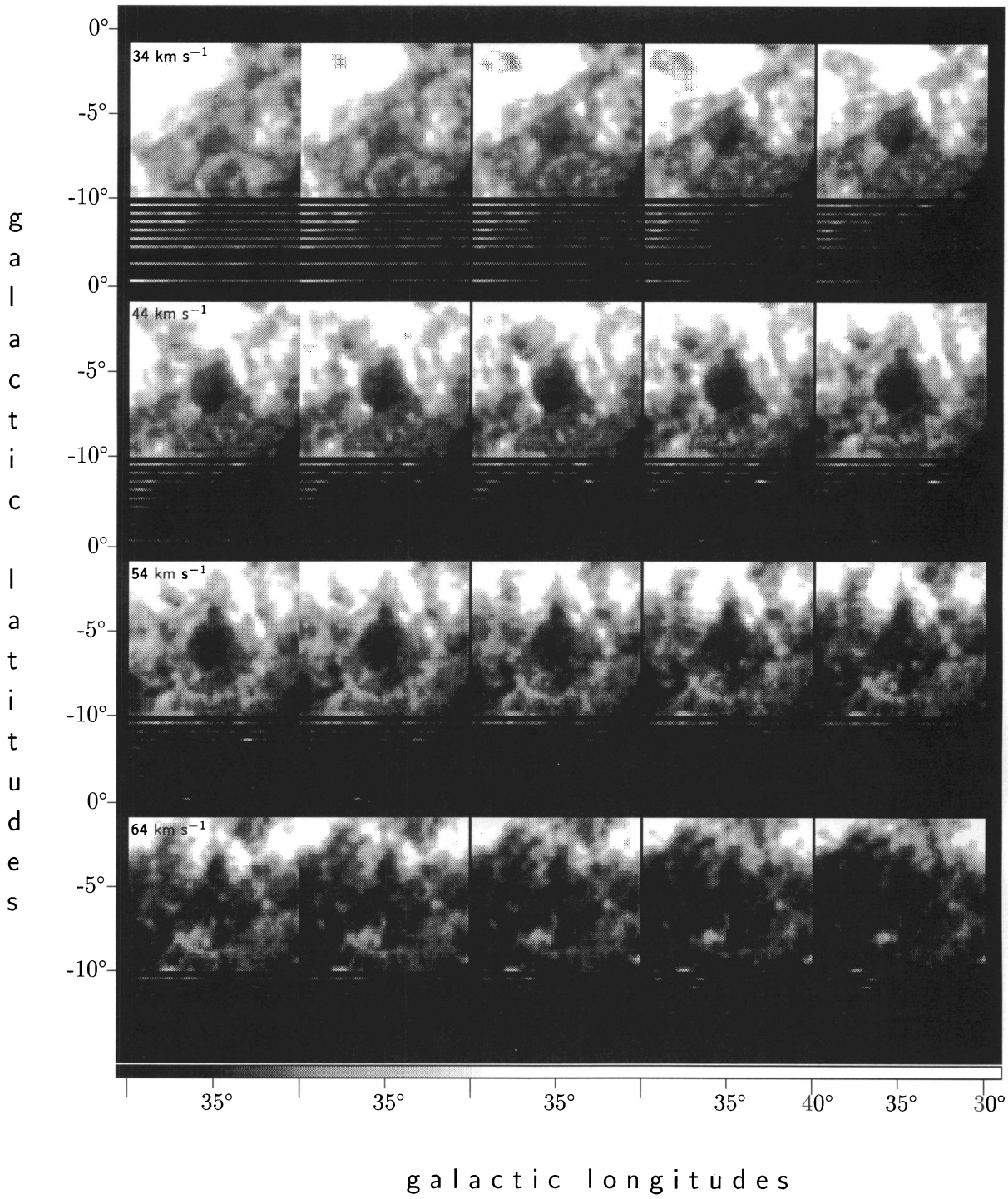

FIG. 2.—A detailed look at the Aquila Supershell: each image displays the H I column density in a region $30° < l < 40°$ and $-15° < b < -1°$ for different LSR radial velocities. Sequence starts from 34 km s^{-1} in the upper left corner to 72 km s^{-1} in the lower right one, with 2 km s^{-1} spacing. Pictures are in a row sequence. Not all latitudes were sampled for $b < -10°$. To increase the dynamic range of this figure, the H I column densities are multiplied by sin $|b|$.

MACIEJEWSKI et al. (see 469, 239)

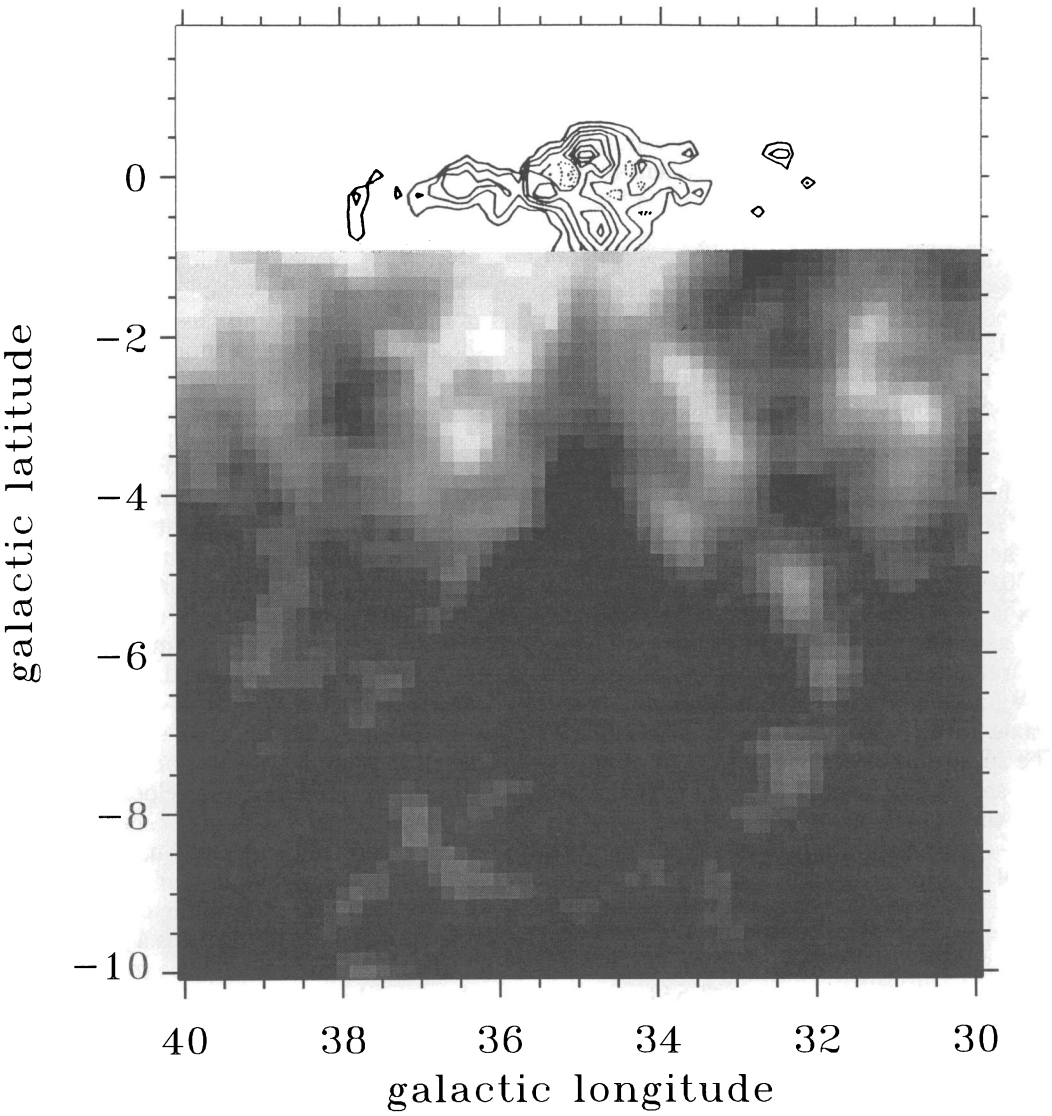

FIG. 3.—H I image of the Aquila Supershell and contours of CO intensity from the [35, 44] molecular cloud. The H I 21 cm emission in a 2 km s^{-1} wide band centered at $v_{LSR} = +56$ km s^{-1} is displayed in gray scale, the cloud CO emission from Dame et al. (1986)—integrated over LSR radial velocities 40–60 km s^{-1}—is in contour representation. CO brightness temperature increases 9.8 K between contours. The H I column densities are multiplied by sin $|b|$.

the image planes 48–70 km s^{-1} and is shifted to lower longitude by $\sim 1°$ from the first part. The opening half angle varies between 25° and 30°. At low velocity, the left lobe of the cone is confused by emission from an H I cloud. At 50 km s^{-1}, the left lobe of the cone looks very different from the right lobe. The left lobe is centered at $l = 36.^{\circ}7$, $b = -1.^{\circ}3$ and extends only to $b = -2.^{\circ}3$, while the right lobe goes to $b = -6.^{\circ}5$. The opening half angle of the left lobe changes monotonically from 60° in this velocity plane to 45° at 56 km s^{-1} and then to 13° at 72 km s^{-1}, where the left lobe is barely detectable.

Between the two lobes of the cone, we observe a very thin channel at $l = 35°$ in the velocity planes 58–64 km s^{-1}. The channel is only 3 pixels (0.°5) wide and extends from $b = -1°$ to $-2.^{\circ}5$. A broader chimney extends from the channel top to $b = -4.^{\circ}0$ in the velocity range 48–68 km s^{-1}.

Figure 4 shows H I spectra in several directions of interest for this system. Note the large velocity width of the emission from the shell, and note the difference in velocity structure of the left and right lobes of the cone. The vertical line marks the adopted systemic velocity of 55 km s^{-1}. The systemic velocity was estimated by finding the velocity at which the gas density within the central 100 pc of the shell interior has a minimum and the gas density in the shell top has a maximum. These two estimates correlate with each other, but one should notice that the estimates bias the adopted velocity toward the velocity of the shell top.

The 55 km s^{-1} systemic velocity implies a kinematic distance to the supershell of either 3.3 kpc or 9.7–10.6 kpc from models of the Galactic rotation curve (Clemens 1985; Rohlfs & Kreitschmann 1987), assuming a Galactocentric distance for the Sun of 8.5 kpc. Because of the probable association of the Aquila Supershell with several H II regions that lie at the near kinematic distance (see § 5.1), we assume that the system lies 3.3 kpc from the Sun. At this distance, 1° corresponds to 58 pc; hence, the Aquila Supershell extends to 550 pc from the Galactic plane, and the maximum radius of the shell is 160 pc. The cone extends up to 370 pc from the Galactic plane.

The sightline toward the Aquila Supershell traverses the Sagittarius arm at the distance between 1.0 and 3.2 kpc

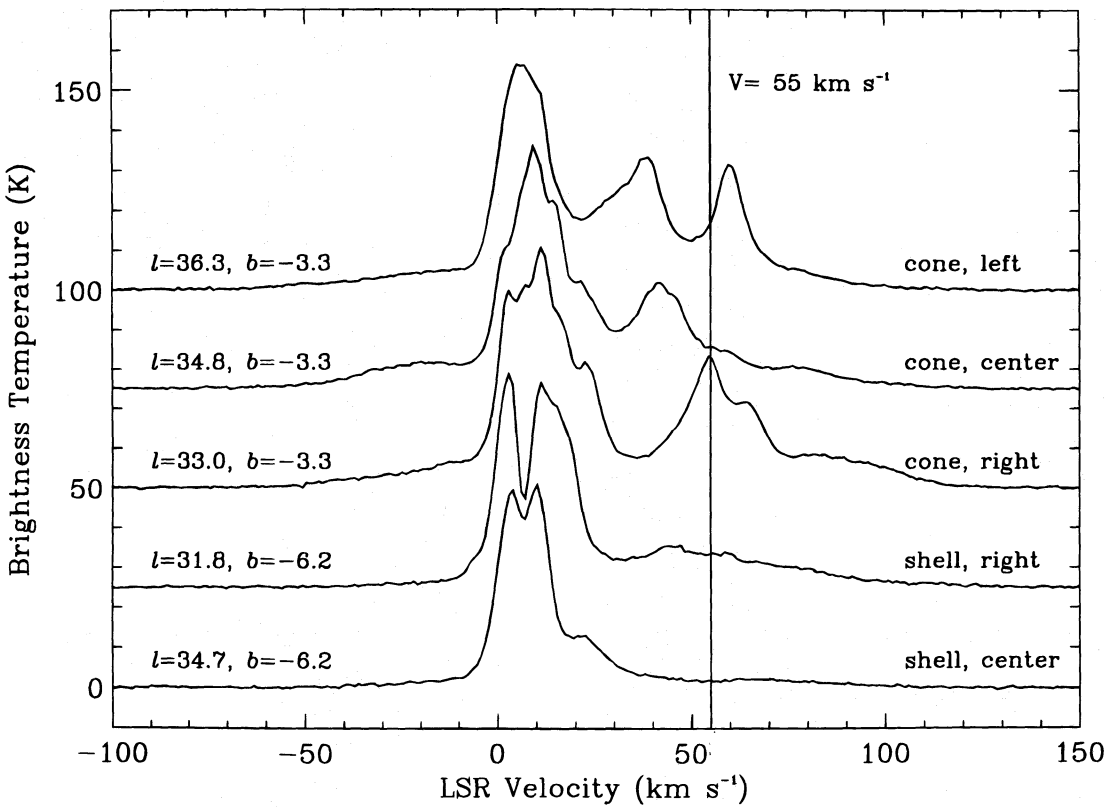

FIG. 4.—Selected 21 cm emission profiles toward the Aquila Supershell. The profile at $l = 34.^{\circ}7$, $b = -6.^{\circ}2$ is in the direction of the center of the shell, and the line of sight toward $l = 31.^{\circ}8$, $b = -6.^{\circ}2$ passes through the edge of the shell. Both of the spectra $l = 33.^{\circ}0$, $b = -3.^{\circ}3$ and $l = 36.^{\circ}3$, $b = -3.^{\circ}3$ are toward sides of the cone, while $l = 34.^{\circ}8$, $b = -3.^{\circ}3$ is toward the center of the cone. The vertical line marks the average velocity of the Aquila Supershell. Velocity resolution is 1 km s^{-1}.

from the Sun (Oort, Kerr, & Westerhout 1958). The position of the remnant imposed on the Oort et al. diagram implies that the Aquila Supershell is located on the inner edge of the Sagittarius arm and that it probably was formed in this arm.

4. MASS, ENERGY, AND AGE

The masses and energies of several shells were determined by Heiles (1979). He estimates that the mass of GS 034−06+65 is $10^6\ M_\odot$, but the low resolution of his survey permits only a simplified mass determination method. Our survey allows for a more detailed method. Heiles estimates that the total energy deposited to GS 034−06+65 is about 1.3×10^{52} ergs. We compare his method of energy determination with numerical models. Comparison with numerical models is also the best method of estimating the age of the supershell.

4.1. *Simple Approach to Mass and Energy Determination*

The mass of the two distinct parts of the Aquila Supershell, the cone and the shell, were calculated separately. For the cone, spectra were integrated between 50 and 72 km s^{-1}, while for the shell, the integration was between 44 and 66 km s^{-1}. A background term that varied with latitude was then subtracted from the integrated column densities. The level of the background was estimated in several ways in order to give upper and lower limits, as well as a best estimate for the system mass. The integrated column density was translated into an H I mass, $M_{\rm H\,I}$, assuming the kinematic distance of 3.3 kpc. The mass estimate depends on the square of this distance. We calculate the total mass by multiplying $M_{\rm H\,I}$ by 1.33 to allow for contributions from elements heavier than hydrogen. The best estimate of mass in the cone is $1.8 \pm 0.4 \times 10^5\ M_\odot$, and in the shell it is $6.0^{+1.6}_{-0.6} \times 10^4\ M_\odot$. We estimate the H I density in the shell interior in a very simplified way. The H I column density at LSR velocity of 55 km s^{-1} in a given direction is divided by the depth of a 2 km s^{-1} slice. Using the Clemens (1985) rotation curve to estimate the distance interval that corresponds to this velocity slice gives an H I density in the shell interior $\sim 1 \times 10^{-2}$ cm^{-3}. To calculate the H I density in the Galactic plane, we extrapolate the density at $b = -1^{\circ}$, assuming a Gaussian stratification with 100 pc scale height so as to obtain a value ~ 1.0 cm^{-3}. These density estimates are extremely uncertain because of a number of factors. For example, turbulence in the gas will smooth out the derived density contrasts. Therefore, the midplane density is probably underestimated and the shell interior density is most likely overestimated.

Heiles (1979) gives an expression for the total energy (kinetic + thermal) required to create a shell that is expanding into a uniform medium and the velocity of which has dropped to 8 km s^{-1}:

$$E_0 = 9.7 \times 10^{44} n_0^{1.12} R^{3.12}\ , \qquad (1)$$

where E_0 is in ergs, n_0 is the ambient H I density in cm^{-3}, and R is the radius of the shell in parsecs. The expansion velocity of the Aquila Supershell parallel to the Galactic plane is much smaller than 15 km s^{-1}, the observed velocity dispersion of the H I lines from the shell; hence, the equation above should be appropriate. The average density of the ambient material swept out by the shell is $n_0 = 0.1$

cm^{-3}, derived by assuming that the shell is a sphere of the radius of $R = 160$ pc and that all of the ambient mass was collected in the shell. Equation (1) then gives an energy deposited into the shell of 5.7×10^{50} ergs. The same procedure applied to the cone, by crudely treating it as a sphere of $\sim 3.^{\circ}3$ diameter with $n_0 = 1.5$ cm^{-3}, gives $E_0 = 2.3 \times 10^{51}$ ergs. The total energy deposited to the Aquila Supershell system would then be about 2.9×10^{51} ergs. The fraction of the energy that was deposited to the cone, evolving in a denser medium, appears here to be larger than the fraction deposited to the shell, which almost freely escapes to the halo. The method used by Heiles was not designed to handle a two-component structure, and we have to reject its result. Heiles's energy derivation is also based on the important assumption that the medium into which the shell expands is uniform. The Aquila Supershell expands from the disk into the halo, where the density is much smaller. The stratification of the medium results in elongated bubbles that can reach greater distances than shells expanding into a uniform medium. On the other hand, the dense medium in the Galactic disk prevents expansion in the disk direction and slows down the early stages of evolution. The best approach to estimate the energy and age of the supershell in these circumstances is to compare the observations with numerical models that have been calculated specifically to describe such systems.

4.2. *Energy and Age Determination from Numerical Models*

Tomisaka & Ikeuchi (1986) give an empirical formula in their equation (20), which allows an estimate for the age t of a supershell. It is based on the numerical models that evolve in a complex stratified disk consisting of two components, interstellar clouds and intercloud medium. They assume constant input of energy of one 10^{51} ergs SN for every 2×10^5 yr. The formula can be written as

$$t = \frac{(z_{up} - z_{es})^{2.3}}{16{,}000} [n(z_{up})]^{0.6} , \qquad (2)$$

where t is in Myr, z_{es} is the height of the energy source, z_{up} is the height of the top of the shell above the Galactic plane in parsecs, and $n(z)$ is the gas density at a given height. For $z_{es} = 0$ and $n(0) = 1.1$ cm^{-3} corresponding to the midplane H I density ~ 1.0 cm^{-3}, which we derived in § 3, the stratification assumed by Tomisaka & Ikeuchi implies $n(550$ pc$) = 4.4 \times 10^{-2}$ cm^{-3}. The age of the Aquila Supershell from equation (2) is then $\sim 2 \times 10^7$ yr, which implies the total (thermal + kinetic) energy input of 1.0×10^{53} ergs, but the models suggest that only about 10^{51} ergs remain as the kinetic energy of the supershell at $t = 2 \times 10^7$ yr. The evident disadvantage of the formula above is the assumed fixed value of the energy input.

The current kinetic energy of the Aquila Supershell can be easily calculated for the cone, where the only velocity comes from the turbulent motion. The kinetic energy of the cone is then $\sim 4 \times 10^{50}$ ergs. The estimation of the current kinetic energy of the shell is much more uncertain. If the expansion of the shell has already stopped, then the shell energy comes from turbulence alone and is $\sim 1.3 \times 10^{50}$ ergs. If the shell still expands to the halo, then the kinetic energy can be as large as $\sim 6 \times 10^{51}$ ergs for a 100 km s^{-1} expansion velocity, which is about the largest possible (Igumentshchev, Shustov, & Tutukov 1990). Therefore, the current kinetic energy of the Aquila Supershell lies roughly between 0.5 and 5×10^{51} ergs, which corresponds well to the Tomisaka & Ikeuchi results.

Mac Low & McCray (1988) and Mac Low, McCray, & Norman (1989) have simulated one 10^{51} erg SN explosion every $(2–3) \times 10^5$ yr in a stratified disk with a midplane density 1–1.3 cm^{-3}. The age of their supershell, which has the size of our object, is $(7–12) \times 10^6$ yr, and the total energy deposited is $(4–4.5) \times 10^{52}$ ergs.

The best way to determine the total energy deposited to the Aquila Supershell is to use a comprehensive set of numerical models with varying energy input rates, such as the one calculated by Igumentshchev et al. (1990). They use a stratified ambient medium with midplane density of 1 cm^{-3}. The remnants with an energy input rate of one 10^{51} ergs SN for every 1.6×10^5 yr reach the observed height of ~ 550 pc at about 8×10^6 yr, with the kinetic energy of 6.5×10^{51} ergs. This energy is at the upper limit of our estimation. On the other hand, the energy input rate must be higher than one SN for every 1.6×10^6 yr because such models do not reach the desired size at all. The total energy input that is required to reach a given height increases with energy input rate; hence, the energy deposited to the supershell is likely to be smaller than 5×10^{52} ergs (the energy deposited to the supershell within 8×10^6 yr, when a 1 SN every 1.6×10^5 yr rate is assumed). It should be larger than 1×10^{52} ergs, corresponding to 1.6×10^7 yr of energy input with the rate of 1 SN for every 1.6×10^6 yr. This allows us to draw the conclusion that the age of the Aquila Supershell is approximately 1×10^7 yr. It is most likely larger than 8×10^6 yr because of the kinetic energy constraint described above. The upper limit of the age depends on how long a nonexpanding shell can survive in the Galactic halo, which is not well determined. The total energy deposited to the Aquila Supershell is in the range $(1–5) \times 10^{52}$ ergs, which corresponds to 10–100 SN explosions, assuming the explosion energy between 0.5 and 1.0×10^{51} ergs. One should notice that the low limit is well defined because lower energy input does not allow expansion of the shell to the desired height. The upper limit is bounded by the vertical expansion velocity of the shell alone, and we cannot estimate this quantity.

The mass of the supershell formed in the models of Igumentshchev et al., 1.25×10^6 $M_{\odot}$, is ~ 5 times larger than what we observe in the Aquila Supershell. Also, the calculated expansion velocity in the Galactic plane, 15 km s^{-1}, is larger than our estimate—it is equal to rms velocity of the turbulent motion. There is no explanation for the first discrepancy, except that we might miss most of the dispersed mass in our estimation because of confusion with nearer and more distant gas. The second discrepancy can be explained by lower energy input rate to the Aquila Supershell than the assumed 1 SN per 1.6×10^5 yr, which results in the 15 km s^{-1} expansion velocity. In such a case, the sizes are the same but the modeled velocity of expansion is larger than the observations.

5. THE PHYSICAL NATURE OF THE AQUILA SUPERSHELL

5.1. *Objects Related to the Aquila Supershell*

There is no evidence of star formation in the shell itself, but there is considerable activity closer to the Galactic plane. Figure 3 shows CO contours of a giant molecular cloud [35, 44] (Dame et al. 1986) that seems highly correlated with the base of the supershell. There is a concentration of H II regions (Lockman 1989) in the field around

longitude 34°–36°.5, presented in Figure 5. Some of them are identified as star formation regions (Plume, Jaffe, & Evans 1992) and compact H II regions (Churchwell, Walmsley, & Cesaroni 1990). Their velocities range from 35 to 64 km s^{-1} and they are found in three velocity groups. Those around 45 km s^{-1} lie at the lowest latitudes, extending to $b = -1°.75$; three of which (W48) appear to lie on the inner surface of the cone and are aligned with the cone lobe. Those in the range 50–56 km s^{-1} are closer to the plane, and all of them have $|b| < 1°$; there are two H II regions with velocity 61–64 km s^{-1}, one of which lies on the cone. The kinematic distance ambiguity for a number of these H II regions can be resolved through use of OH, H_2CO, or H I absorption spectra (see Turner 1979; Downes et al. 1980; Kuchar & Bania 1994). All but one of these H II regions are at the near kinematic distance; thus, from this association we conclude that the Aquila Supershell is also likely at its near kinematic distance of 3.3 kpc. Of the 12 H II regions between 34° and 36° longitude, only two lie above the Galactic plane (and then just a few tenths of a degree), while the remaining 10 lie below the plane, some to nearly −2° latitude. It appears that all recent star formation in this part of the Galaxy is displaced to negative z.

There are several SN remnants detected in this area—G34.7−0.4, G35.6−0.4 (Milne 1979); G33.6+0.0 (Kes79), G33.2−0.6, G36.6−0.7 (Green 1988; Kassim 1989, 1992); G35.0−1.1 (Kistiakowsky & Helfand 1993)—but only G34.7−0.4 (W44; Rho et al. 1994) seems likely to be associated with the supershell. W44 on Figure 5 is an oval-shaped enhancement of continuum emission at the base of the cone. Absorption in its direction shows several spectral features at velocities 42–55 km s^{-1}, and several distance determination methods give the result $d = 3.0$–3.5 kpc. W44 is a shell remnant of a Type II supernova (McKee, van Buren, & Lazareff 1984) with a noticeable deviation from spherical symmetry, indicating nonuniformity of the medium into which it expands. Both the simplest model of W44 (Shelton et al. 1996) and the age of the pulsar in its interior (Wolszczan, Cordes, & Dewey 1991) imply that W44 is about 20,000 yr old. One can also notice that stronger radio continuum emission, indicating higher density of the ambient medium into which the remnant evolves, comes from the part of W44 that is located on the extension of the cone lobe. It also overlaps with the densest part of the [35, 44] molecular cloud. The pulsar inside W44 is displaced about 5′ south of the geometric center of the remnant. This may be explained either by a large (~200 km s^{-1}) projected velocity of the pulsar or by a lack of symmetry of the remnant expanding in a nonuniform medium. The W44 continuum emission gradient suggests that the remnant expands in the direction perpendicular to the cone. The observation of a cometary compact H II region G34.3+0.2, the tail of which is directed exactly outward from the remnant (Reid & Ho 1985), can be explained by winds blowing out of an active star formation region around W44. The two pulsars that were detected next to W44 may indicate a strong star formation activity there.

A good tracer of recent nucleosynthesis activity is the 1.809 MeV emission line produced in the decay of ^{26}Al. The emission from the Galactic plane in this line was mapped with the COMPTEL imaging telescope (Diehl et al. 1995), with angular response ~4° FWHM, resulting in an angular accuracy for the stronger features of ~1°. In addition to strong emission from the Galactic center, there is a second-

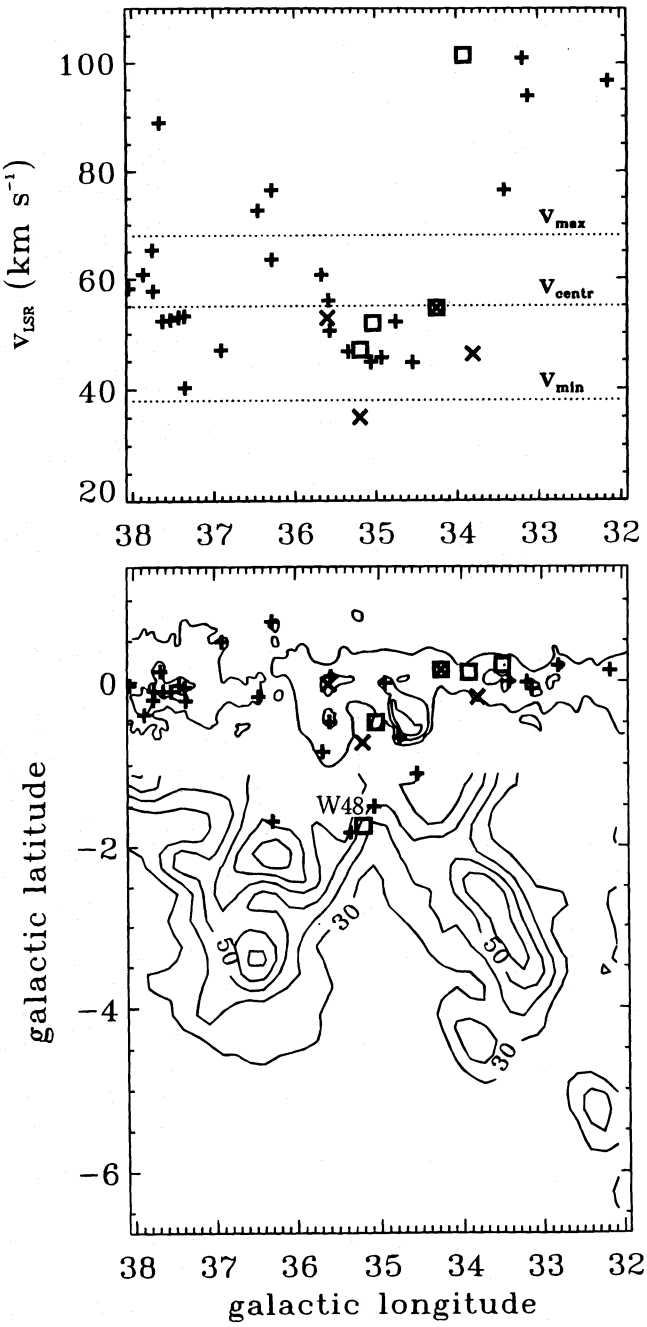

FIG. 5.—Distribution of H II regions in the base of the Aquila Supershell. *Lower graph*: the 21 cm emission contours are plotted in solid line for $b < -1°$. Contours correspond to the H I emission in a 2 km s^{-1} wide band centered at $v_{LSR} = +56$ km s^{-1}. Numbers correspond to H I column densities multiplied by $\sin|b|$ in 10^{17} cm^{-2}. Contours for $b > -1°$ schematically outline the continuous radio emission at 6 cm wavelength. They are based on the Altenhoff et al. (1978) survey. The cone shape is reproduced in continuum emission. Notice the vertical elongation of H II regions near the base of the cone. The "+" symbols correspond to H II regions, "×" symbols represent star formation regions, and squares are compact H II regions. *Upper graph*: the distribution of H II regions with LSR velocity. Notice the concentration around $l = 35°$, $v_{LSR} = 50$ km s^{-1}. Three horizontal dotted lines correspond to maximum, central, and minimum LSR velocity of the Aquila Supershell.

ary enhancement at $l = 33°$, $b = 0°$. There is no known emission source in this direction, except the Scutum arm edge, but this edge is more likely responsible for weaker emission at $l < 33°$. The star formation regions in the [35, 44] molecular cloud are, therefore, likely to be the source,

and the emission from the Scutum arm may be responsible for the shift of maximum emission toward low Galactic latitudes. If it is true, other unidentified 1.809 MeV emission regions may be good places to look for Galactic supershells. Nevertheless, since the emission at $l = 33°$, $b = 0°$ is much stronger than emission in any other direction except the Galactic center, the Aquila Supershell might not be a typical structure in the Galaxy.

5.2. *X-Ray Emission*

The *ROSAT* All-Sky Survey (Snowden et al. 1995), with its 2° resolution and very sharp point-spread function, has detected a region of diffuse X-ray emission in the 0.75 and 1.5 keV bands, which partially overlaps with the Aquila Supershell. Emission at levels higher than 250×10^{-6} counts s^{-1} $arcmin^{-2}$ extends from $l = 33°$ to $l = 38°$ and from $b = -2°$ to $b = -9°$ in the 0.75 keV band. For the 1.5 keV band with the same count threshold, the X-ray emission extends over $32° \leq l \leq 37°$, $-7° \leq b \leq 0°$. In this area, the Galactic background emission is 150×10^{-6} counts s^{-1} $arcmin^{-2}$.

The emission from the southwest and northeast parts of the shell is attenuated and anticorrelated with H I column densities in this direction. There are two possible sources of the extended emission from this region, in addition to the supershell interior: Loop I and the Galactic center. Nonetheless, the termination of the X-ray emission at the upper boundary of the supershell favors the hypothesis that the emission comes from the shell interior. At a distance of 3.3 kpc, we expect there to be foreground H I toward the shell center with a column density greater than 10^{21} cm^{-2}, which corresponds to the optical depths more than 0.4 in the 0.75 keV band and more than 0.1 in the 1.5 keV band. Therefore, there can be significant foreground attenuation of X-rays from the shell, and we expect the attenuation to vary strongly with latitude. The X-ray emission from a supershell containing hot gas strongly depends on the properties of the ambient medium. However, the observed emission is roughly consistent with X-ray emission from 10^6 to 10^7 K gas, which is expected to reside in evolved multiple SN remnants (Silich et al. 1994).

5.3. *Scenario of Structure Formation and Related Events*

Our observations of the Aquila Supershell, as well as the information about the region in the Galactic disk underlying this remnant, allow us to hypothesize about physical processes operating there and to propose a scenario of events that may have occurred. The molecular cloud complex [35, 44] is the most probable primary site of star formation activity in this region. Virtually all star formation occurs at negative latitudes; hence, the center of Type II SN explosions most likely occurred below the Galactic plane, perhaps up to $z \sim -100$ pc. The hot gas produced by stellar winds and SN explosions likely formed a bubble separated by a shock wave from the ambient medium. The main part of the molecular cloud halted the expansion of the bubble toward positive latitudes. The ambient gas was compressed into a structure with a conelike shape at low latitudes. This shape is not fully theoretically understood yet. The models predict the existence of a cylindrical chimney of vertical walls at low latitudes, which connects to the shell of similar radius in the halo (e.g. Tenorio-Tagle, Różyczka, & Bodenheimer 1990), and do not predict the narrowing of the walls toward the Galactic plane, which we observe. The existence of the cone can be explained by an energy source of the supershell located 200–300 pc away from the Galactic plane (Mac Low, McCray, & Norman 1989), but this would require that star formation in this part of the Galaxy proceeded sequentially from the lower halo toward the Galactic plane. The cone can also be formed when a hot bubble breaks out from a dense cloud into a low-density ambient medium (Tenorio-Tagle, Różyczka, & Yorke 1985). However, this scenario requires a large density contrast, ~100 times larger than the observed one. The cone formed in the models is small, irregular, and not very dense. The cone on Figure 3 is larger than the cloud itself, and its mass is ~0.1 the mass of the cloud.

One of the most intriguing features of the Aquila Supershell is the thin channel between the cone lobes. This channel connects the remnant interior to the active star formation region, and its morphology is more jetlike than chimney-like. We have no explanation for this feature. The compression of the ambient gas in the cone evidently was large enough to trigger secondary star formation, which is likely to occur in W48. The alignment of W48 H II regions parallel to the east lobe of the cone, as described in § 5.1, suggests that they formed from one cloud after the shock outlining the cone had passed through it.

The X-ray diffuse emission detected in the *ROSAT* All-Sky Survey indicates that the gas inside the supershell is still very hot. In § 3, we implied that the shell may not have broken into the halo. If the shell were evolving into hot halo gas, the expansion velocity of the shell would be smaller than the speed of sound. No shock would surround the shell, which would therefore break into the halo. The relatively coherent top shell suggests that the gas above the shell in the halo must be cold enough so that the expansion of the shell remains supersonic. The shell is surrounded by the shock, which prevents gas mixing between the hot interior of the shell and the surrounding halo. Any hot halo gas in the surroundings of the Aquila Supershell must lie above the height of 600 pc. Nevertheless, these conclusions are not definite because geometrical and dynamical effects can make the interpretation of velocity images very misleading. Simple models constructed by us, in which an empty cylinder of a given wall thickness and with no top was immersed in the disk, often resulted in artificial features, including an apparent top of the cylinder in a velocity image.

If active star formation in the [35, 44] molecular cloud has persisted for 10^7 yr, then the SN production rate required to form the supershell is not large; one SN for every $(0.2–1) \times 10^6$ yr will supply the energy required to reach the observed height. W44 and other SN remnants in the region may be examples of recent explosive contributions to the supershell.

The ~5 km s^{-1} discrepancy between the velocity of the supershell center and the average velocities of the H II regions and the [35, 44] molecular cloud (Fig. 5*a*) can have several origins. First, the visibility of the supershell is worse at lower velocities because of foreground contamination; thus, the central velocity of the Aquila Supershell may appear to be higher than it really is. Second, there may exist a vertical gradient in the velocity of the supershell, which actually can be traced on Figure 2: the top of the shell is more visible at high velocities, the cone is more visible at low velocities. Since, as we mentioned in § 3, the supershell velocity is biased toward the top of the shell, we conclude that if the velocity gradient is real, the supershell velocity is

overestimated. Finally, the origin of velocity discrepancy may be in large mass concentration under the supershell. The gas after crossing a spiral arm moves faster than before entering the arm because of gravitational attraction of the arm. The gas is also shocked in the arm, which causes rapid velocity changes. Both of these effects are most important close to the mass concentration; hence, a velocity difference may appear between the gas in the plane and the gas out of the plane in the close neighborhood of the [35, 44] molecular cloud. The larger the mass of the cloud is, the more visible the effect should be.

It is interesting to compare the Aquila Supershell with the recently discovered "H I chimney" in Perseus (Normandeau, Taylor, & Dewdney 1996). The chimney appears as a void in H I maps, surrounded by faint Hα emission wisps (Topasna, Dennison, & Simonetti 1995). The wisps extend vertically from a young stellar cluster associated with W4 up to the height of 230 pc above the Galactic plane, where they appear to close. The Aquila Supershell extends approximately twice as far into the halo.

6. SUMMARY

Our observation of the Aquila Supershell suggests that it is a remnant caused by the collective action of SN explosions and stellar winds originating in a star-forming region that is associated with a molecular cloud. The explosive activity has lasted for about 10^7 yr, and the energy deposited to the supershell equals that of about 10–100 SN explosions. In the early stage of the activity, collective wind and SN events from massive stars produced a primary shock wave. The shock compressed the ambient gas into a cone and triggered star formation there. Continuous activity taking place in the molecular cloud at the base of the cone gave the shock wave an energy large enough to escape to the halo and to form a spherical shell there. The star formation activity in the molecular cloud still persists today, which is indicated by sequential SN explosions in a partially processed medium and by a strong ^{26}Al gamma-ray emission. The system has several mysteries, including a relatively intact upper part of the shell, a narrow channel connecting the cone to the molecular cloud, and an internal velocity structure whose meaning is not clear.

W. M. and B. D. S. acknowledge support from NASA grant NAG 5-1852.

REFERENCES

Altenhoff, W. J., Downes, D., Pauls, T., & Schraml, J. 1978, A&AS, 35, 23
Brinks, E., & Bajaja, E. 1986, A&A, 169, 14
Churchwell, E., Walmsley, C. M., & Cesaroni, R. 1990, A&AS, 83, 119
Clemens, D. P. 1985, ApJ, 295, 422
Dame, T. M., Elmegreen, B. G., Cohen, R. S., & Thaddeus, P. 1986, ApJ, 305, 892
Deul, E. R., & den Hartog, R. H. 1990, A&A, 229, 362
Diehl, R., et al. 1995, A&A, 298, 445
Downes, D., Wilson, T. L., Bieging, J., & Wink, J. 1980, A&AS, 40, 379
Green, D. A. 1988, Ap&SS, 148, 3
Heiles, C. 1979, ApJ, 229, 533
———. 1984, ApJS, 55, 585
Igumentshchev, I. V., Shustov, B. M., & Tutukov, A. V. 1990, A&A, 234, 396
Kamphuis, J., Sancisi, R., & van der Hulst, T. 1991, A&A, 244, L29
Kassim, N. E. 1989, ApJS, 71, 799
———. 1992, AJ, 103, 943
Kistiakowsky, V., & Helfand, D. J. 1993, AJ, 105, 2199
Koo, B.-C., Heiles, C., & Reach, W. T. 1992, ApJ, 390, 108
Kuchar, T. A., & Bania, T. M. 1994, ApJ, 436, 117
Lockman, F. J. 1989, ApJS, 71, 469
Mac Low, M.-M., & McCray, R. 1988, ApJ, 324, 776
Mac Low, M.-M., McCray, R., & Norman, M. L. 1989, ApJ, 337, 141
McCray, R., & Kafatos, M. 1987, ApJ, 317, 190
McKee, C. F., van Buren, D., & Lazareff, B. 1984, ApJ, 278, L115
Milne, D. K. 1979, Australian J. Phys., 32, 83
Normandeau, M., Taylor, A. R., & Dewdney, P. E. 1996, Nature, 380, 687
Oort, J. H., Kerr, F. T., & Westerhout, G. 1958, MNRAS, 118, 379
Plume, R., Jaffe, D. T., & Evans, N. J., II. 1992, ApJS, 78, 505
Reid, M. J., & Ho, P. T. P. 1985, ApJ, 288, L17
Rho, J., Petre R., Schlegel, E. M., & Hester, J. J. 1994, ApJ, 430, 757
Rohlfs, K., & Kreitschmann, J. 1987, A&A, 178, 95
Shapiro, P. R., & Field, G. B. 1976, ApJ, 205, 762
Shelton R., et al. 1996, in preparation
Silich, S. A., Franco, J., Palous, J., & Tenorio-Tagle, G. 1994, in Numerical Simulations in Astrophysics, ed. J. Franco et al. (Cambridge: Cambridge Univ. Press), 193
Snowden, S. L., et al. 1995, ApJ, in press
Tenorio-Tagle, G., & Bodenheimer, P. 1988, ARA&A, 26, 145
Tenorio-Tagle, G., Franco, J., Bodenheimer, P., & Różyczka, M. 1987, A&A, 179, 219
Tenorio-Tagle, G., Różyczka, M., & Bodenheimer, P. 1990, A&A, 237, 207
Tenorio-Tagle, G., Różyczka, M., & Yorke, H. W. 1985, A&A, 148, 52
Tomisaka, K., & Ikeuchi, S. 1986, PASJ, 38, 697
Topasna, G. A., Dennison, B., & Simonetti, J. H. 1995, BAAS, 27, 1348
Turner, B. E. 1979, A&AS, 37, 1
Williams, D. R. 1973, A&AS, 8, 505
Wolszczan, A., Cordes, J. M., & Dewey, R. J. 1991, ApJ, 372, L99